Supporting Information

Salicylate 5-Hydroxylase: Intermediates in Aromatic Hydroxylation by a Rieske Monooxygenase

Melanie S. Rogers and John D. Lipscomb*

Department of Biochemistry, Molecular Biology, and Biophysics
and the Center for Metals in Biocatalysis
University of Minnesota, Minneapolis, Minnesota 55455, United States

Supporting Information Table of Contents

SUPPLEMENTAL EXPERIMENTAL PROCEDURES

Cloning of Tagless S5HH. *Ralstonia* sp. strain U2 genes for S5HH (*nagGH*) were cloned from pWWF6.[1, 2] Cloning oligonucleotides used for PCR amplification are shown in Table S1. Restriction sites are bolded and underlined. Following digest with the appropriate restriction enzymes, constructs were ligated into similarly cut over-expression plasmids. The resulting constructs were verified by sequencing at the University of Minnesota Genomics Center. *E. coli* strains DH5α and BL21(DE3) were used for cloning and over-expression, respectively.

Table S1. Cloning Oligonucleotides and Plasmids Used to Produce Tagless S5HH

Cloning oligonucleotides	**Sequence** (restriction sites bolded and underlined)
NDE I S5H for p29	GC**CATATG**ATGAGTGAACCCCAACGATT
ECOR I S5H rev p29	GC**GAATTC**TCAGATTGGATAGATCACAG
Plasmids	**Description**
pWWF6	pUC18 containing *Ralstonia* sp. strain U2 *nag* genes [1, 2]
pACYC-*isc*	pACYC-Duet containing part of the *E. coli isc* operon /P15A origin / chloramphenicol resistant [3]
pET29b(+)	pET plasmid with thrombin cleavage site / pBR322 origin / kanamycin resistant[a]
pS5HH-*tagless*	pET29 plasmid containing *Ralstonia* sp. strain U2 *nag* genes *nagGH*

[a]Novagen, Madison, USA

Heterologous Expression of Tagless S5HH. S5HH was over-expressed using the following procedure. *E. coli* BL21(DE3) was co-transformed with pS5HH-*tagless* and pACYC-*isc*. Liquid starter cultures were grown using LB media with kanamycin (50 μg/ml) and chloramphenicol (34 μg/ml). A single colony was transferred to 5 ml media, incubated for 6 h (37 °C, 250 rpm) then 40 μl was used to inoculate 500 ml media which was grown overnight (28 °C, 150 rpm). The overnight culture was used to inoculate TB-glycerol media (1 L) containing kanamycin (50 μg/ml), chloramphenicol (34 μg/ml) and ferrous ammonium sulfate (15 μM). Baffled 2-L flasks were used and 1 drop of Antifoam 204 (Sigma-Aldrich) was added. Cultures were incubated at 30 °C, 150 rpm. When OD_{600} ~ 1.3 was reached, ferrous ammonium sulfate was added (15 μM) and the culture was cooled to 16 °C, then IPTG (600 μM) was added. After 16 h, cells were harvest by centrifugation, the cell paste was washed with 10 mM MOPS, pH 7.0 and then stored at -80 °C.

Purification of Tagless S5HH. Tagless S5HH cell paste (60 g) was suspended in 20 mM MOPS, 5 % glycerol, 1 mM DTT, pH 7.5 buffer (180 ml) containing DNAseI (5 mg) and lysozyme (10 mg) and then stirred (4 °C, 20 min). The cell suspension was lysed by sonication as described in Experimental Procedures. All subsequent procedures were performed at 4 °C. The lysate was centrifuged at 75,600 RCF_{max} for 1 h. Cold water (250 ml) was added to the cell-free extract to lower the conductivity of the solution. The diluted solution was applied (5 ml/min) to a 500 ml DEAE Sepharose FF (GE Healthcare Lifesciences) purification resin equilibrated with 20 mM MOPS, 5 % glycerol, 1 mM DTT, pH 7.5 buffer. The column was washed (1 L) with the same buffer followed by elution using a 3 L gradient from 0 mM to 0.5 M NaCl (12 ml/min). Fractions were screened via UV-visible spectroscopy, conductivity and SDS-PAGE and the selected fractions were pooled. To prepare for hydrophobic interactions chromatography, ammonium sulfate solution (3 M) was added to the pooled fractions to 1 M final concentration. The resulting solution, which remained clear, was applied (10 ml/min) to a 115 ml Octyl Sepharose (GE Healthcare Lifesciences) purification resin equilibrated with 25 mM BisTris, 5 % glycerol, 1 M ammonium sulfate, 1 mM DTT, pH 6.8 buffer. The column was washed (2 L) with buffer containing 0.8 M ammonium sulfate followed by elution with a buffer gradient (2 L) from 0.8 M to 0 M ammonium sulfate (12 ml/min). Fractions were screened via UV-visible spectroscopy and SDS-PAGE. Pooled S5HH protein fractions were concentrated using an Amicon pressure-driven device (30 kDa cut-off) and then a centrifugal concentration device (30 kDa cut off). The resulting tagless S5HH protein (100 mg, 550 μM) was aliquoted, flash-frozen in liquid nitrogen and stored at -80 °C. At the conclusion of this purification method, tagless S5HH contained an approximately stoichiometric oxidized Rieske cluster but no ferrous mononuclear iron per $\alpha\beta$ protomer.

Anaerobic Technique and Chemical Reduction of S5HH. Solutions were deoxygenated using a Schlenck line. Protein solutions were deoxygenated by flowing oxygen-scrubbed ultra-high purity argon gas through the headspace of a stirred solution (4 °C) in a sealed vial. Stirred buffer solutions in sealed serum bottles (Wheaton) were deoxygenated by sparging with argon gas (23 °C). The Rieske cluster of S5HH was chemically reduced via incubation (5 min) of an anaerobic solution with sodium dithionite (4.5 mM) and methyl viologen (200 μM). Dithionite and methyl viologen were removed using a PD-10 desalting column (GE Healthcare Lifesciences). Chemical reduction was performed in a Coy anaerobic chamber. The reduced S5HH was subsequently used in single-turnover (STO) reactions.

HPLC Product Analysis. HPLC was performed on a Waters system with a 1525 binary pump, 2487 dual-wavelength UV/vis detector (230 nm), and an Agilent Zorbax SB C18 column (4.6 mm × 150 mm, 5 μm) with a 1 ml injection loop. Mobile phase A: acetonitrile, 0.1 % formic acid. Mobile phase B: water, 0.1 % formic acid. Samples were loaded at 4 % A and eluted with a linear gradient of 4 to 30 % A over 5.4 min then 30 to 100 % A over 3.8 min at 2.5 ml/min. RCQ gentisate product quantitation was performed with a caffeic acid internal standard and data were analyzed according to Magee and Herd.[5]

LC-MS Product Analysis. LC separation of single-turnover samples was achieved on a Waters Acquity ULPC with a 2.1 x 100 mm Waters Acquity HSS T3 C18 (1.7 μM particle size) column, 10 μL loop, 5 μL injection volume. Mobile phase A: water, 0.1 % formic acid and mobile phase B: acetonitrile, 0.1 % formic acid. Samples were injected at 97 % A and eluted over a linear gradient to 3 % A from 5 min to 15 min at 0.4 ml/min. Mass spectral detection was via a Waters Synapt G2 UPLC/QTOF-MS.

Mass spectrometry analysis was performed at The University of Minnesota Department of Chemistry Mass Spectrometry Laboratory (MSL), supported by the Office of the Vice President of Research, College of Science and Engineering, and the Department of Chemistry at the University of Minnesota, as well as The National Science Foundation (NSF, Award CHE-1336940). The content of this paper is the sole responsibility of the authors and does not represent endorsement by the MSL or NSF.

Stopped-Flow Measurements and Analysis. Single-wavelength measurements or photodiode array measurements of steady-state or single-turnover reactions were made using an Applied Photophysics SX.18MV spectrophotometer. For a linear series of first order or pseudo-first order reactions, the time course can be fit by summing exponential expressions where the number of exponentials is equal to the number of steps, n (Eq. 1). If the steps are irreversible, then the reciprocal relaxation times ($1/\tau$) give the rate constants for individual steps, although it is not possible to assign a specific reciprocal relaxation time to the rate constant for a specific step without additional information. When the steps are reversible,

the reciprocal relaxation times become coupled so that they do not correlate with a specific rate constant. In some cases, the rate constants can be determined from the ligand concentration dependence of the reciprocal relaxation times.[6]

$$Abs_t = (\sum_{i=1}^{n} Amp_i\, e^{-\frac{t}{\tau i}}) + Abs_{inf} \qquad \text{(Eq. 1)}$$

The kinetic data were fit to Eq. 1 using the nonlinear regression function of the Applied Photophysics ProData Viewer program. In this equation, Abs_t is the observed absorbance at time t, Amp_i is the observed amplitude for exponential phase i, τ_i is the relaxation time for phase i, and Abs_{inf} is the final absorbance at the end of the reaction. Fitting statistics were reported by the fitting program, and each reaction was repeated multiple times (see specific experiment) to determine the average fitting parameters and errors.

For a two-step reaction where the first step is fast, reversible ligand binding (Eq. 2), only one exponential phase may be observed. A plot of $1/\tau_{obs}$ versus the concentration of the binding ligand will be hyperbolic if the rate constant k_{-1} is at least 3 fold greater than k_2 (Eq. 3).[7]

$$\text{E + ligand} \underset{k_{-1}}{\overset{k_1}{\rightleftarrows}} \text{E·ligand} \underset{k_{-2}}{\overset{k_2}{\rightleftarrows}} \text{E-ligand'} \qquad \text{(Eq. 2)}$$

$$\frac{1}{\tau_{obs}} = \frac{k_2[\text{ligand}]}{(\frac{k_{-1}}{k_1})+[\text{ligand}]} + k_{-2} \qquad \text{(Eq. 3)}$$

The parameters of the equation yield the apparent K_D for the binding reaction (k_{-1}/k_1) and forward and reverse rate constants for observable conversion which follows binding. The accuracy of the K_D value depends upon how closely the binding reaction approaches rapid equilibrium, and specifically, whether the above cited relationship of k_{-1} and k_2 is valid.

EPR Measurements. X-band EPR spectra were recorded with a Bruker ELEXSYS E500 instrument equipped with an Oxford ESR910 liquid helium cryostat. The spectra were plotted, simulated, and integrated using the program SpinCount created by Michael P. Hendrich, Carnegie Mellon University.[8] At the end of a single-turnover reaction before product dissociation, the mononuclear iron of S5HH exhibits an EPR spectrum from an $S = 5/2$ spin system. This spectrum was analyzed using a spin Hamiltonian equation Eq. 4.[9, 10]

$$\hat{\mathcal{H}} = D\left[\hat{S}_z^2 - \frac{35}{12} + \left(\frac{E}{D}\right)\left(\hat{S}_x^2 - \hat{S}_y^2\right)\right] + g_0\beta\hat{\boldsymbol{S}}\bullet\mathbf{B} + \hat{\boldsymbol{I}}\bullet\boldsymbol{A}\bullet\hat{\boldsymbol{S}} \qquad \text{(Eq. 4)}$$

In this equation, D and E are the tetragonal and rhombic zero field splitting (ZFS) parameters and (x,y,z) designate the principal axes of the ZFS tensor. The term $\boldsymbol{A}$, is the transferred hyperfine coupling tensor of the ^{17}O-ligand, when a ligand enriched in ^{17}O is bound to the iron. The other parameters have their usual definitions. The final term in the equation describes the interaction of the electron spin with the I = 5/2 nuclear spin of the ^{17}O ligand. In principle, it would result in splitting of the EPR resonances, but the splitting is not resolved in the spectra reported here, and the effect is observed as a broadening of the signal. The term E/D is a measure of the departure of the electronic environment of the iron from axial symmetry and can assume values between 0 and 1/3, the extreme values representing the axial and completely rhombic cases, respectively. In practice, the E/D value is determined from the observed ground state and excited state EPR resonances and the use of either SpinCount [8] or the program Visual RHOMBO.[11] The value of E/D establishes the ZFS in multiples of D. For the S = 5/2, E/D = 0.333 system studied here, the splitting energy is 3.5 D between both the ground (m_s = ±1/2) and middle (m_s = ±3/2) Kramers doublets and the middle and upper (m_s = ±5/2) doublets. Measurement of the relative populations (intensity) of the resonances from the states at two or more temperatures allows the value of D to be approximated by fitting to the Boltzmann distribution and correcting for the Curie Law (1/T) dependence of the resonance intensity.[12] Eq. 5 gives the relative intensity N of the middle doublet where k_b is the Boltzmann constant.[13]

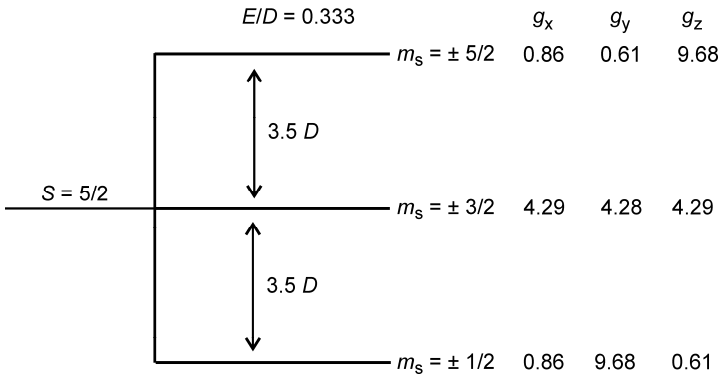

$$\boldsymbol{N_{g=4.3} \propto \frac{1}{T}\left[\frac{e^{-3.5D/k_bT}}{1+e^{-3.5D/k_bT}+e^{-7D/k_bT}}\right]} \qquad \text{(Eq. 5)}$$

The half saturation power of the g = 4.3 EPR signal ($P_{1/2}$) was determined by systematically increasing the microwave power (P) from a non-saturating to a saturating value and observing the peak to trough signal intensity (S_N). The $P_{1/2}$ is given by the breakpoint of the plot:[14]

$$\boldsymbol{log\left(\frac{S_N}{\sqrt{P}}\right) vs. log\,(P)} \qquad \text{(Eq. 6)}$$

Quantification of the g = 4.3 Species. The g = 4.3 species was quantified by double integration of the resonance in comparison with the similar resonance from protocatechuate 3,4-dioxygenase (3,4-PCD).[10]. The spectra of a trapped sample from the S5HH single turnover reaction at 3 s (Figure 7) and a 3,4-PCD sample of known metal site concentration were recorded at 7 K and doubly integrated. After correction for occupancy of the middle Kramers state using the D values for each enzyme (see Figure S4; D for 3,4-PCD = 1.6 cm^{-1}),[13] the concentration for the g = 4.3 species in S5HH was calculated.

SUPPLEMENTAL FIGURES

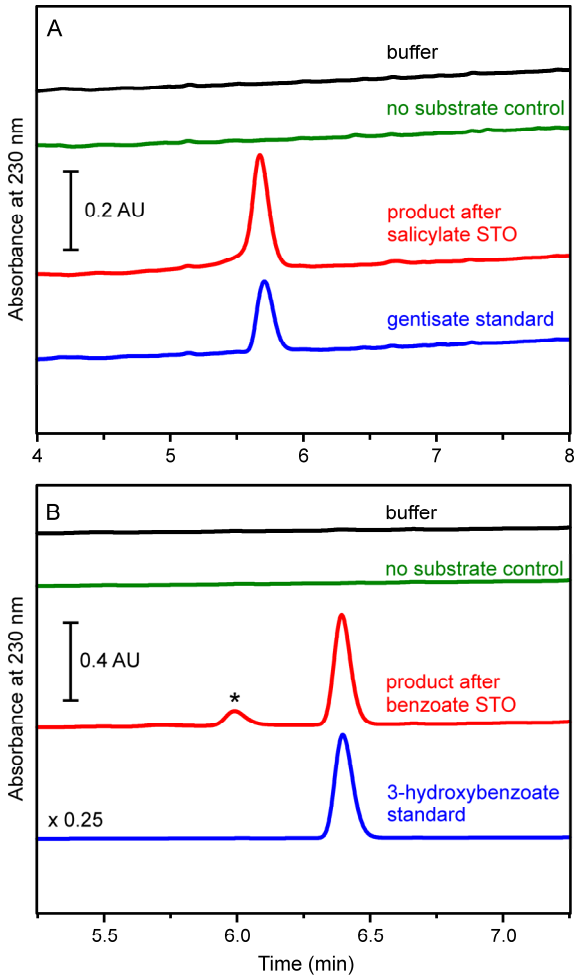

Figure S1. HPLC product analysis of a single-turnover reaction of S5HH with salicylate or benzoate. Fully reduced S5HH (207 µM) was reacted with (A) salicylate (8.41 mM) or (B) benzoate (9 mM), and oxygen (900 µM) in 200 mM HEPES, 100 mM NaCl, 5 % glycerol, pH 8.0 (concentrations after mixing). After 1 hour at 23 °C, the reaction was quenched (1:1) with 10 % TFA while vortexing, and then 1 M HEPES pH 8.0 was added (1:1 with added TFA solution volume) to the quenched sample. Precipitated enzyme was removed via centrifugation. Authentic gentisate and 3-hydroxybenzoate product standards were prepared and quenched in the same manner. The elution peak marked with a * in panel B is a contaminant in the benzoate stock.

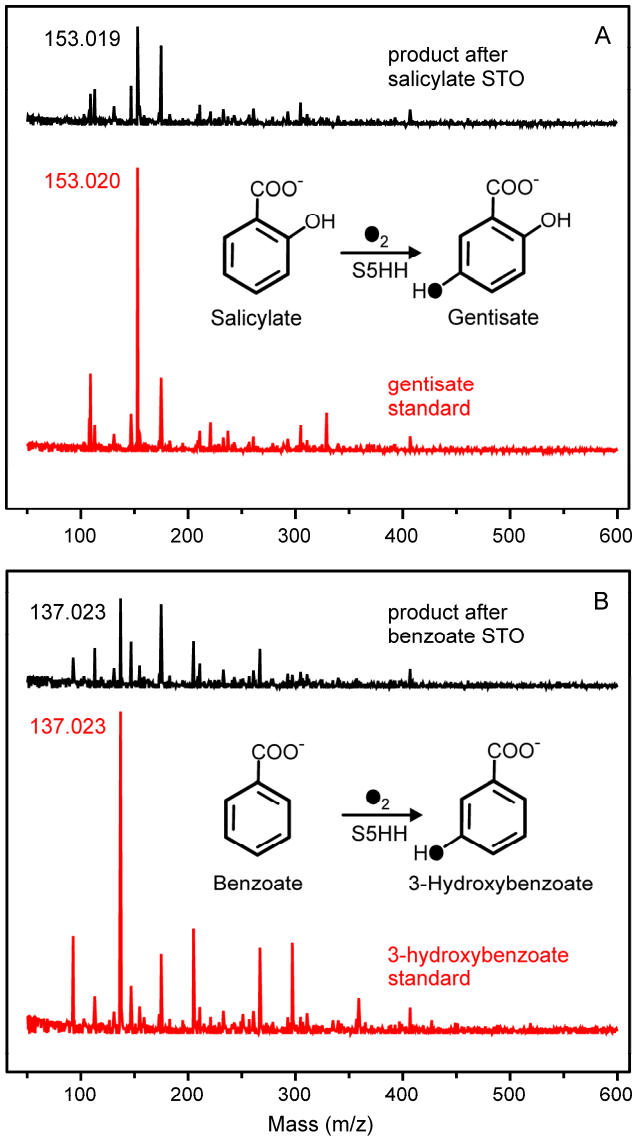

Figure S2. LC-MS product analysis of a single-turnover reaction of S5HH with salicylate or benzoate. Mass spectra of completed and extracted (A) salicylate reaction (LC peak at 9.332 s), or (B) benzoate reaction (LC peak at 9.659 s). Single-turnover reactions performed as described in Figure S1.

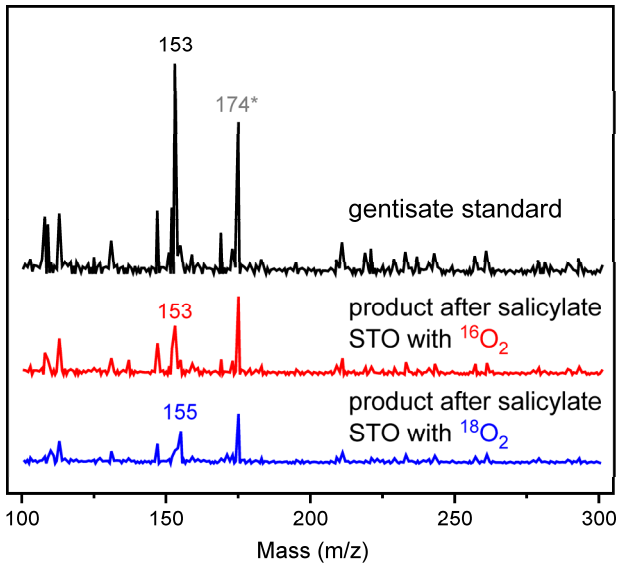

Figure S3. LC-MS product analysis of a single turnover reaction of S5HH with $^{18}O_2$ and salicylate. Mass spectra of completed and extracted reaction with $^{16}O_2$ (red), or $^{18}O_2$ (blue) and gentisate product standard (black). The peak at 174 marked with a * originates from a non-S5HH-related background signal. Fully reduced S5HH (178 µM) was reacted with salicylate (37.5 mM), and either with $^{16}O_2$ (900 µM) or with $^{18}O_2$ (900 µM) in 200 mM HEPES, 100 mM NaCl, 5 % glycerol, pH 8.0 buffer (concentrations after mixing). After 1 hour at 23 °C, the reaction was quenched (1:1) with 10 % TFA while vortexing, and then 1 M HEPES pH 8.0 (1:1 with TFA volume) was added to the quenched sample. Precipitated enzyme was removed via centrifugation. An authentic gentisate product standard (50 µM) was prepared and quenched in the same manner.

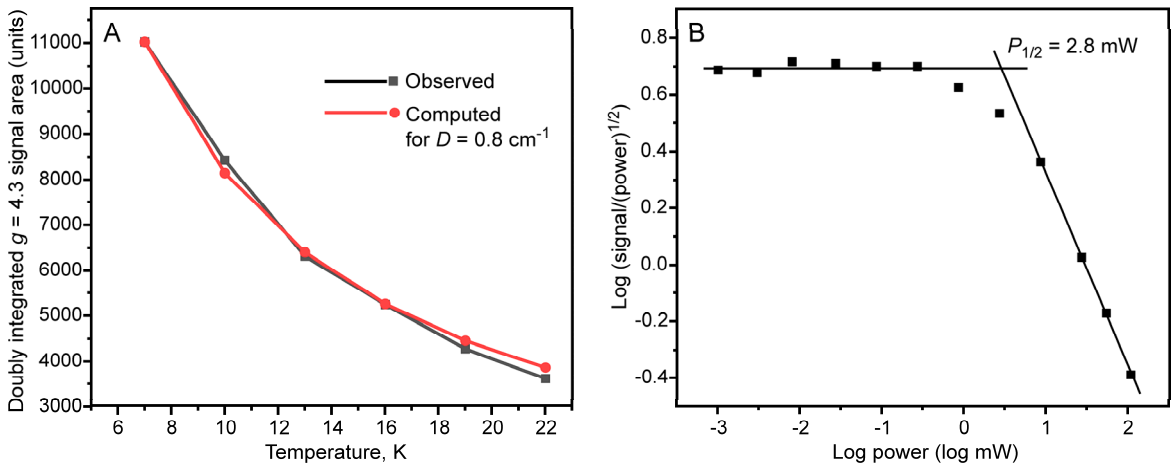

Figure S4. Estimation of the zero field splitting parameter D and $P_{1/2}$ for the $g = 4.3$ species present after product forms in a single turnover reaction of S5HH. (A) The signals recorded over the temperature range shown were doubly integrated (black) using SpinCount. The predicted integrated area for $D = 0.8$ cm^{-1} computed using Eq. 5 and normalized to the area for the 7 K data is shown in red. (B) The microwave power was increased over the range shown at T = 1.9 K and the peak to trough signal intensity of the g = 4.3 plotted according to Eq. 6.

SUPPLEMENTAL DISCUSSION

Special Assay Conditions for S5H Required Due to Low K_m and k_{cat} Values. The low $K_{M\ salicylate}$ and k_{cat} for S5H complicated the measurement of the kinetic parameters, which could easily lead to artifacts. This problem stems from the requirement that the substrate concentration be much greater than the enzyme concentration to satisfy the conditions for fitting via the Michaelis Menten equation. For S5H, when sufficient enzyme is supplied to observe turnover in a typical benchtop spectrophotometer or polarograph chamber, the requisite large excess of substrate pushes the enzyme into saturation. Similar behavior was also observed for NDO.[4] This problem was addressed here through the use of a stopped-flow spectrophotometer to allow rapid, thorough mixing and high absorption sensitivity, so that accurate initial velocities and turnover of very low concentrations of S5HH at salicylate concentrations near the K_M could be accurately monitored. The ratio of S5HR, S5HF, and S5HH used in these experiments was chosen by individually testing the amount of each protein required to achieve maximal enzyme activity in the assay under these conditions.

Origin of the Multiple Phases in the Summed-Exponential Fit to the Single Turnover Time Course. It is argued in the main text that the phases observed in the single turnover time courses originate from either parallel or sequential irreversible reactions. Consequently, it is possible to associate $1/\tau$ values with rate constants for the steps. The fastest phase of the salicylate single turnover time course at 453 nm, $1/\tau_1$, correlates with the rate constant for electron transfer from the Rieske cluster and product formation. The $1/\tau_2$ at 453 nm is slower than formation of the 700 nm Fe(III)-product complex, but it is much faster than autooxidation, so this low amplitude phase may represent electron transfer to a mononuclear iron site that has bound oxygen and substrate but cannot complete the turnover reaction. $1/\tau_3$ is the weighted average of the two slow Rieske autooxidation rate constants, so this phase may represent electron transfer to external acceptors for sites that have a Rieske cluster but no mononuclear iron. All three of these processes are nearly complete (~ 95% based on the $1/\tau$ values in Table 2) by the time the 700 nm species has fully formed. The optical spectrum at this stage in the 350-600 nm region is very similar to that of as-isolated S5HH at the same concentration, consistent with $\geqslant$ 95% oxidation of the Rieske cluster. The fastest $1/\tau_1$ value of the reaction at 700 nm is likely to represent the rate constant for formation of the Fe(III)-product complex, which occurs more slowly than product is formed in the active site. The low amplitude second phase may reflect optical changes due to the autooxidation of Rieske cluster, but its true origin remains unknown. At 700 nm, $1/\tau_3$ is assigned as the rate constant for product release from the mononuclear iron (loss of the 700 nm species). This step occurs with the formation of an isosbestic point at 575 nm and increase in absorbance at 453. We originally assigned this increase to further slow oxidation of the Rieske

cluster, but this would imply that there is a substantial amount of reduced Rieske present. If this were the case, we would expect a spectral shift during the 3 to 1000 s period (as in the 0 to 3 s period), which is not observed. Two potential explanations for the observed isosbestic point and lack of a spectral shift are: (i) the ferric mononuclear site has an broad absorbance in the 450 nm region when product is not bound or (ii) release of the product allows a shift in the position of the mononuclear iron, which in turn alters the environment and extinction coefficient of the Rieske cluster. At present, we cannot resolve these possibilities.

SUPPLEMENTAL REFERENCES

[1] Keenan, B. G., Leungsakul, T., Smets, B. F., Mori, M.-a., Henderson, D. E., and Wood, T. K. (2005) Protein engineering of the archetypal nitroarene dioxygenase of *Ralstonia* sp. strain U2 for activity on aminonitrotoluenes and dinitrotoluenes through alpha-subunit residues leucine 225, phenylalanine 350, and glycine 407, *J. Bacteriol. 187*, 3302-3310.

[2] Fuenmayor, S. L., Wild, M., Boyes, A. L., and Williams, P. A. (1998) A gene cluster encoding steps in conversion of naphthalene to gentisate in *Pseudomonas* sp. strain U2, *J. Bacteriol. 180*, 2522-2530.

[3] Tiwari, M. K., Lee, J. K., Moon, H. J., and Zhao, H. (2011) Further biochemical studies on aminopyrrolnitrin oxygenase (PrnD), *Bioorg Med Chem Lett 21*, 2873-2876.

[4] Jouanneau, Y., Meyer, C., Jakoncic, J., Stojanoff, V., and Gaillard, J. (2006) Characterization of a naphthalene dioxygenase endowed with an exceptionally broad substrate specificity toward polycyclic aromatic hydrocarbons, *Biochemistry 45*, 12380-12391.

[5] Magee, J. A., and Herd, A. C. (1999) Internal standard calculations in chromatography, *J. Chem. Educ. 76*, 252.

[6] Groce, S. L., Miller-Rodeberg, M. A., and Lipscomb, J. D. (2004) Single-turnover kinetics of homoprotocatechuate 2,3-dioxygenase, *Biochemistry 43*, 15141-15153.

[7] Whittaker, J. W., and Lipscomb, J. D. (1984) Transition state analogs for protocatechuate 3,4-dioxygenase. Spectroscopic and kinetic studies of the binding reactions of ketonized substrate analogs, *J. Biol. Chem. 259*, 4476-4486.

[8] Petasis, D. T., and Hendrich, M. P. (2015) Quantitative interpretation of multifrequency multimode EPR spectra of metal-containing proteins, enzymes, and biomimetic complexes, *Methods Enzymol. 563*, 171-208.

[9] Palmer, G. (2000) Electron paramagnetic resonance of metalloproteins, In *Physical Methods in Bioinorganic Chemistry* (Que Jr., L., Ed.), pp 121-185, University Science Books, Sausalito, CA.

[10] Que, L., Jr., Lipscomb, J. D., Zimmermann, R., Münck, E., Orme-Johnson, N. R., and Orme-Johnson, W. H. (1976) Mössbauer and EPR spectroscopy of protocatechuate 3,4-dioxygenase from *Pseudomonas aeruginosa*, *Biochim. Biophys. Acta 452*, 320-334.

[11] Hagen, W. R. (2007) Wide zero field interaction distributions in the high-spin EPR of metalloproteins, *Mol. Phys. 105*, 2031-2039.

[12] Liu, L. V., Hong, S., Cho, J., Nam, W., and Solomon, E. I. (2013) Comparison of high-spin and low-spin nonheme Fe(III)-OOH complexes in O-O bond homolysis and H-atom abstraction reactivities., *J. Am. Chem. Soc. 135*, 3286-3299.

[13] Que, L., Jr., Lipscomb, J. D., Münck, E., and Wood, J. M. (1977) Protocatechuate 3,4-dioxygenase. Inhibitor studies and mechanistic implications, *Biochim. Biophys. Acta 485*, 60-74.

[14] Lipscomb, J. D. (1980) Electron paramagnetic resonance detectable states of cytochrome P-450$_{cam}$, *Biochemistry 19*, 3590-3599.